"Liquid Metals" and the relation to "Warm Dense Matter"

Friedrich Hensel

WDM: Interest in the dramatic changes in electronic behavior that can develop under large changes of thermodynamic variables.

Remarkable example: The pressure induced ionization in the nominally nonmetallic fluids H_2, N_2, O_2, He

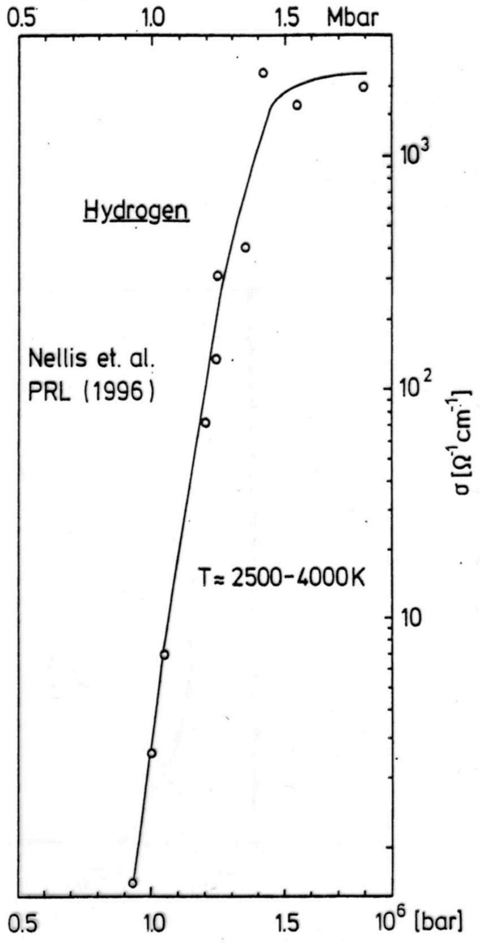

However, major questions regarding these fluids such as precise equation of state determination, knowledge of the molecular structure and of special importance the existence of the „plasma phase transition“ and the location of its critical point are still unsolved. The unfavorable outlook for measurements in the critical region of the PPT in the WDM-region has motivated the application of “molecular dynamics simulations” and has led to renewed interest in the phase behavior of fluid metals, because fluid metals are examples *par excellence* of materials whose electronic structure and properties depend strongly on the thermodynamic state of the system.

b)

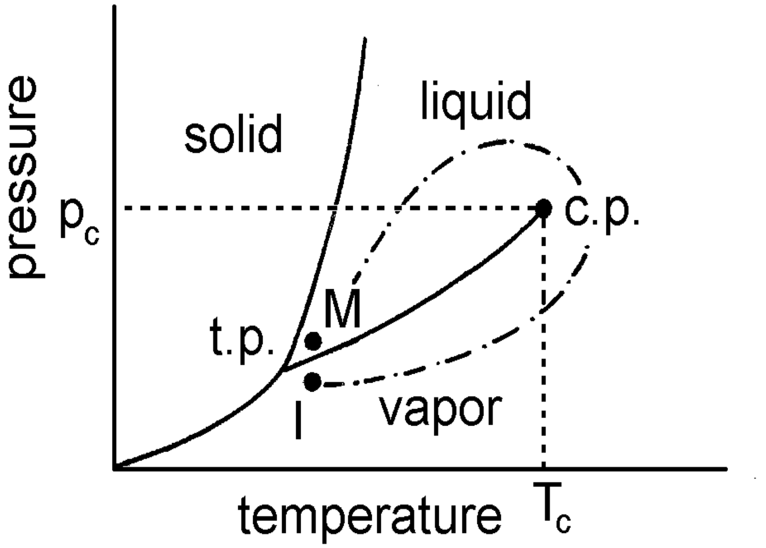

Landau, Zeldovitch, Acta Phys. Chem. USSR **18**, 194 (1943)

c)

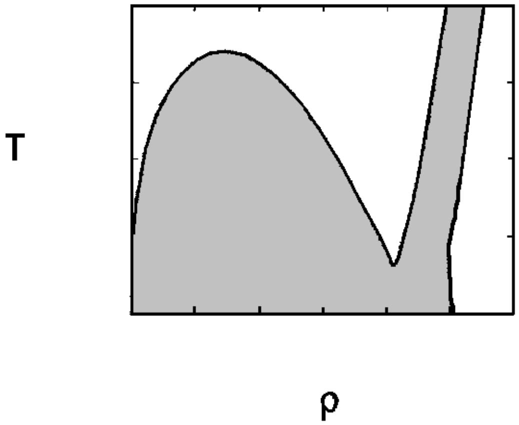

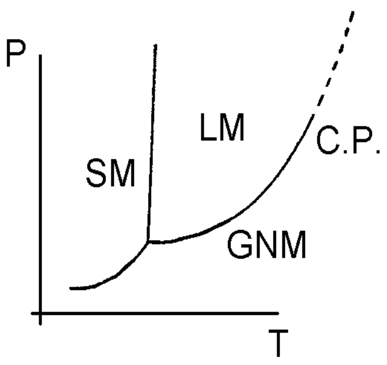

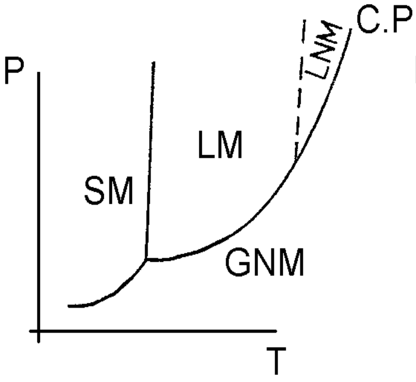

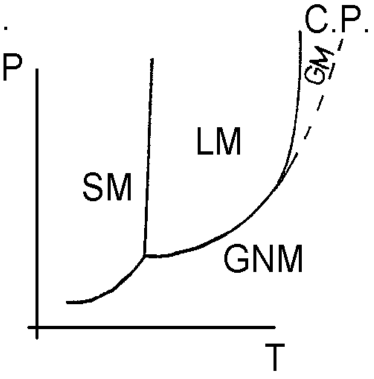

Critical Data of Fluid Metals

	Metal	T_c / °C	p_c / bar	ρ_c / g cm^{-3}
static	Mercury	1478	1673	5.80
	Cesium	1651	92.5	0.38
	Rubidium	1744	124.5	0.29
	Potassium	1905	148	0.18
WDM	Sodium	2210	248	0.30
	Lithium	3000	690	0.11
	Lead	5100	2500	3.20
	Indium	6700	4000	2.10
	Molybdenum	14000	570	2.90

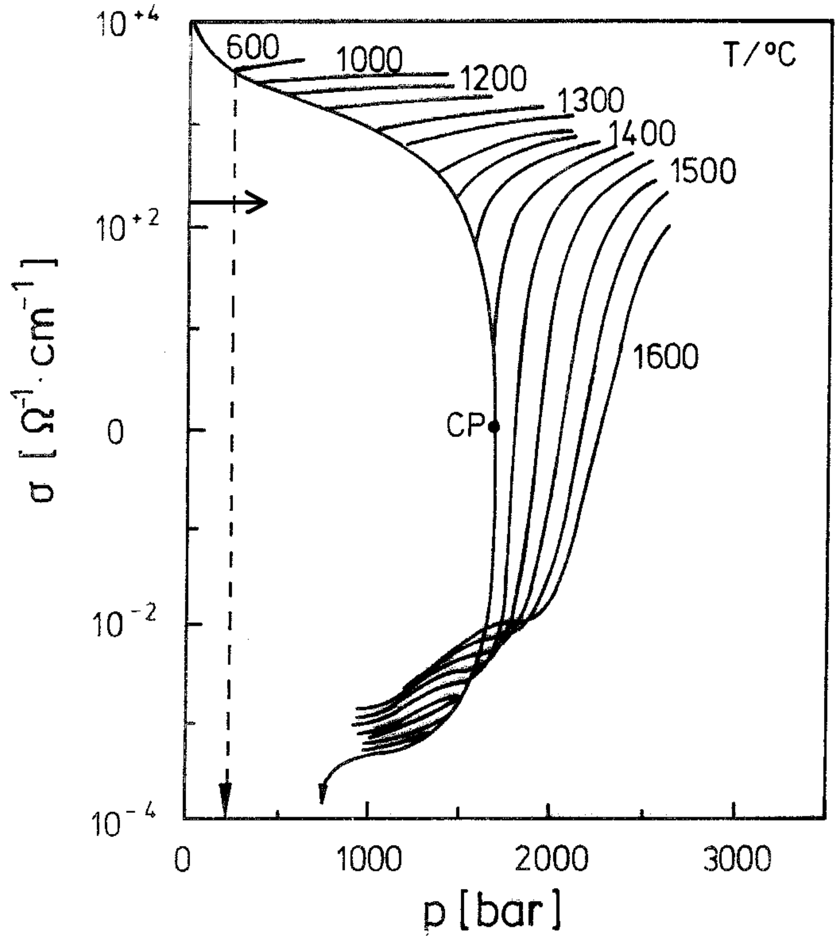
10^+4
10^+2
0
10^-2
10^-4
σ [Ω^-1 · cm^-1]
0
1000
2000
3000
p [bar]
T/°C
600
1000
1200
1300
1400
1500
1600
CP

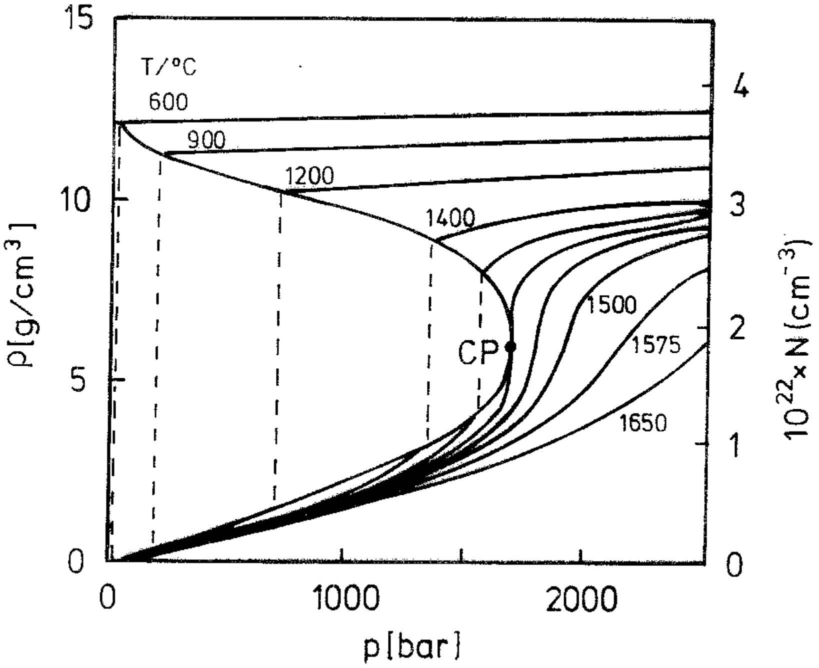
15
10
5
0
ρ[g/cm^3]
4
3
2
1
0
10^22 × N(cm^-3)
0
1000
2000
p[bar]
T/°C
600
900
1200
1400
1500
1575
1650
CP

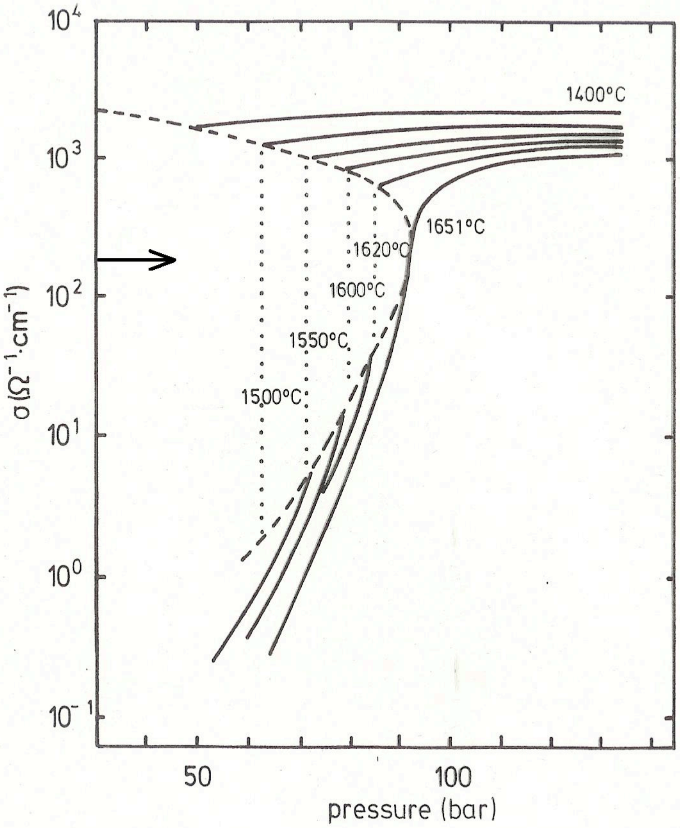

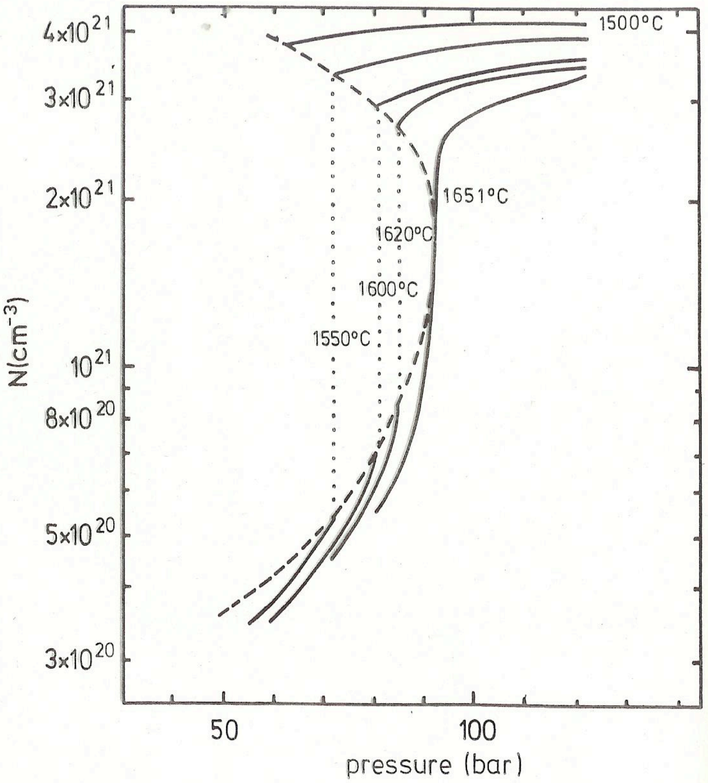

No rigorous criterion to distinguish metal from nonmetal above absolute zero of temperature

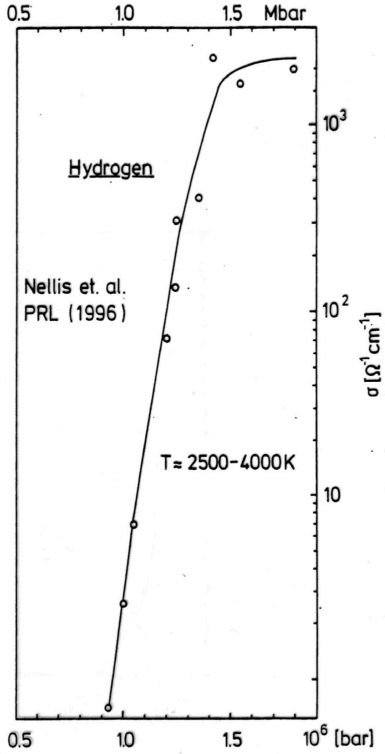

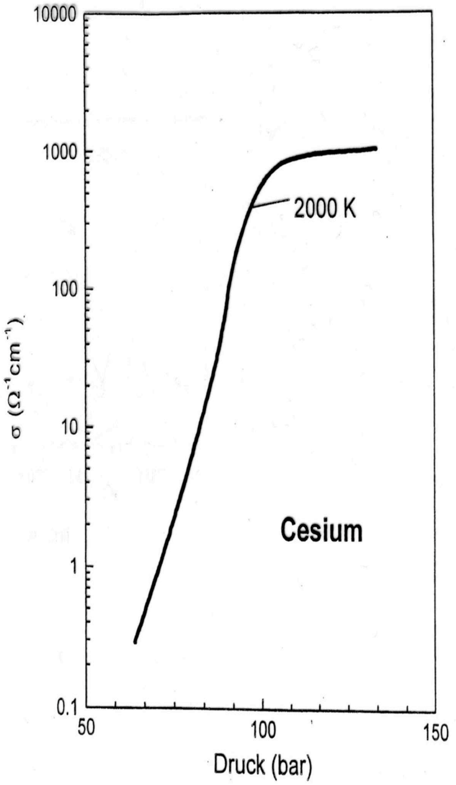

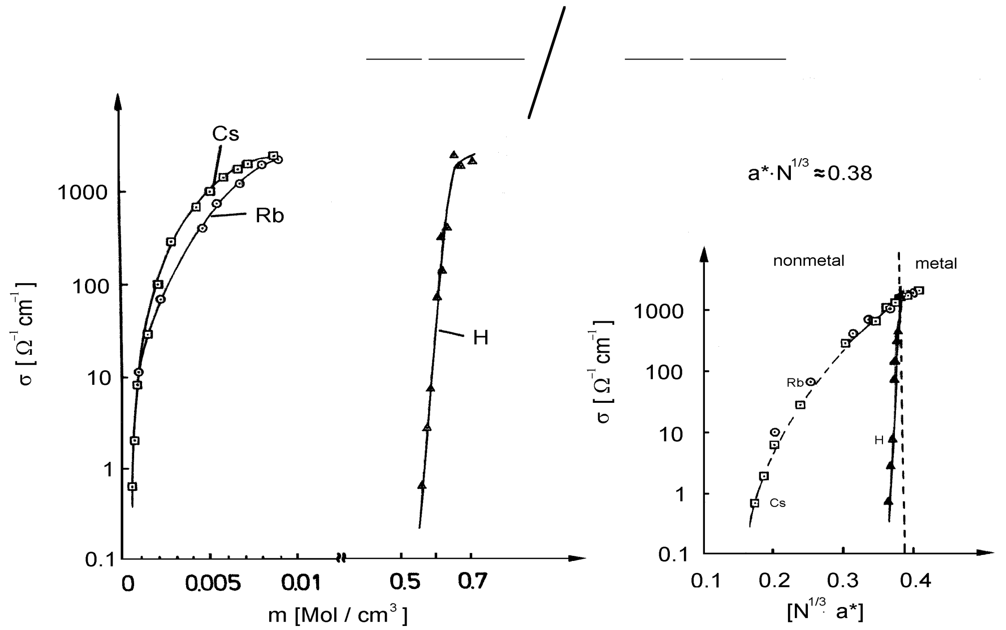

(Hensel and Nellis APS 1996)

Survival of the strong chemical bond in H_2 ?

Physical models suggest that significant concentrations of neutral dimers and dimer ions exist under WDM-conditions in Hydrogen

Prove: QMD-simulations and comparison with the Structural properties of the experimentally accessible Fluid alkali metals

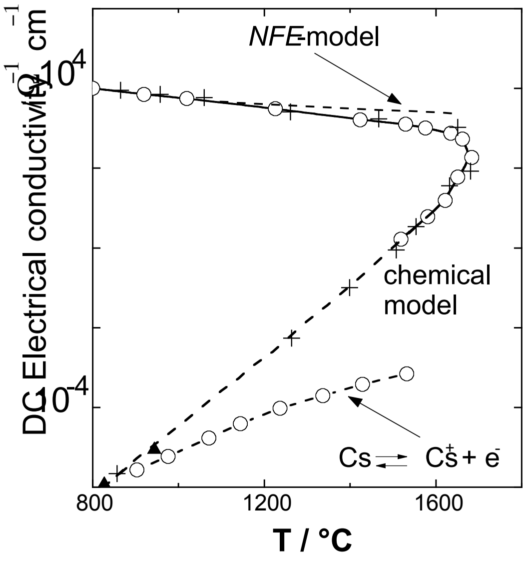

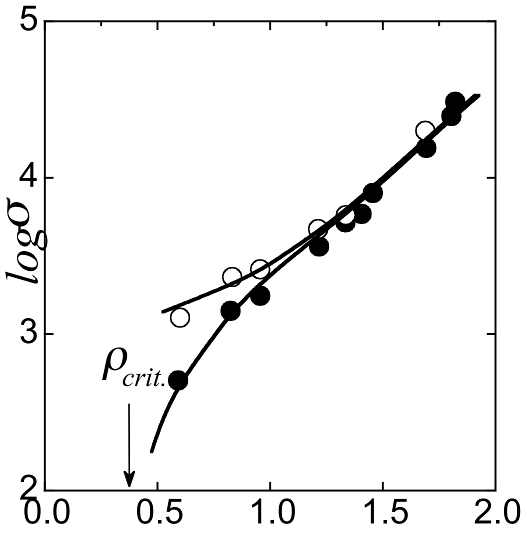

Rubidium

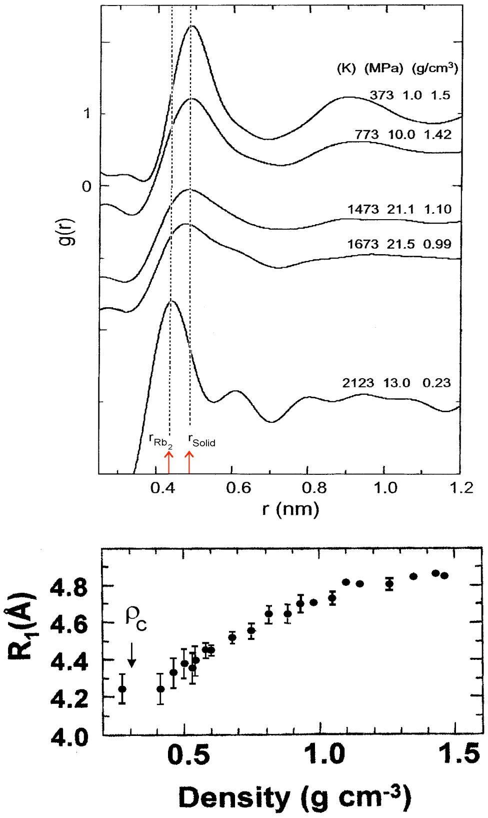

K. Matsuda et al., J. Non-Cryst. Sol. in press (2006)

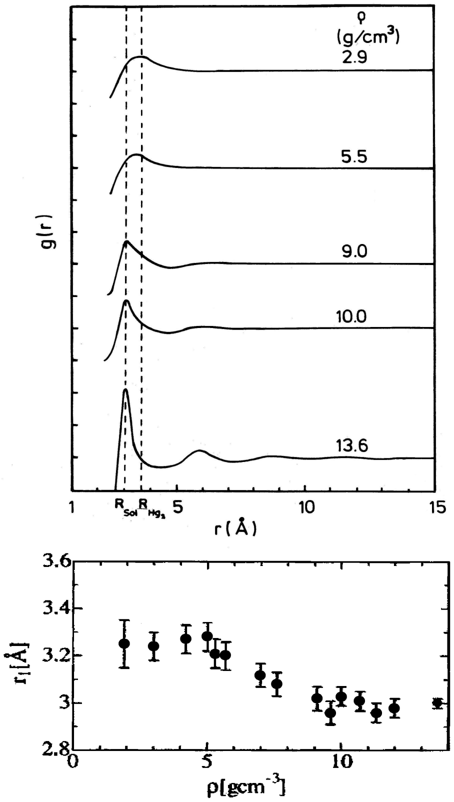

Inui et al., PRB **68**, 094108 (2003)

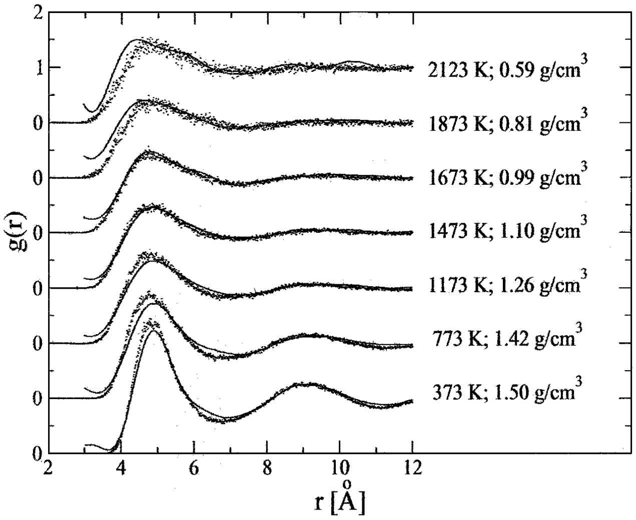

Figure 2. Pair correlation function for expanded fluid Rb: QMD simulations (data points) are compared with x-ray diffraction experiments (solid lines) [4].

Quantum Molecular Dynamics Simulations for Expanded Fluid Rb und Cs

A. Kietzmann, R. Redmer
Institut für Physik, Universität Rostock, D-18051 Rostock, Germany

M. P. Desjarlais, T. R. Mattson
Pulsed Power Sciences Center, Sandia National Laboratories, Albuquerque, NM 87185

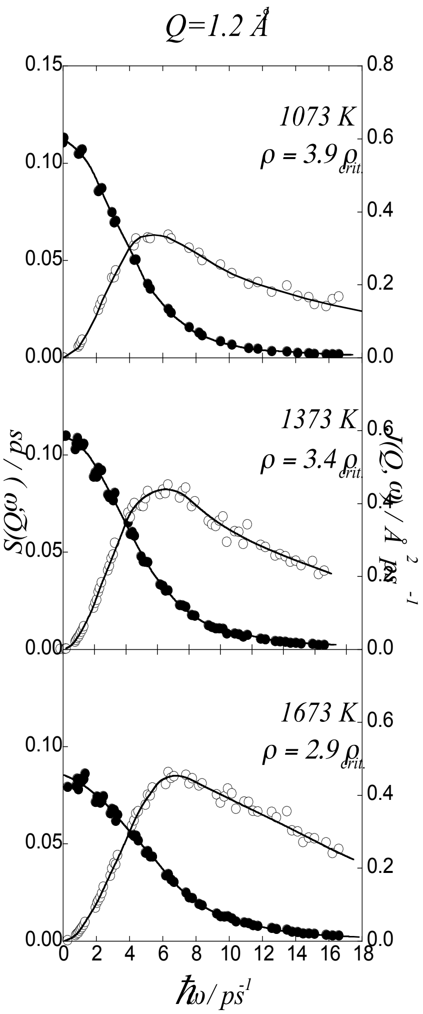

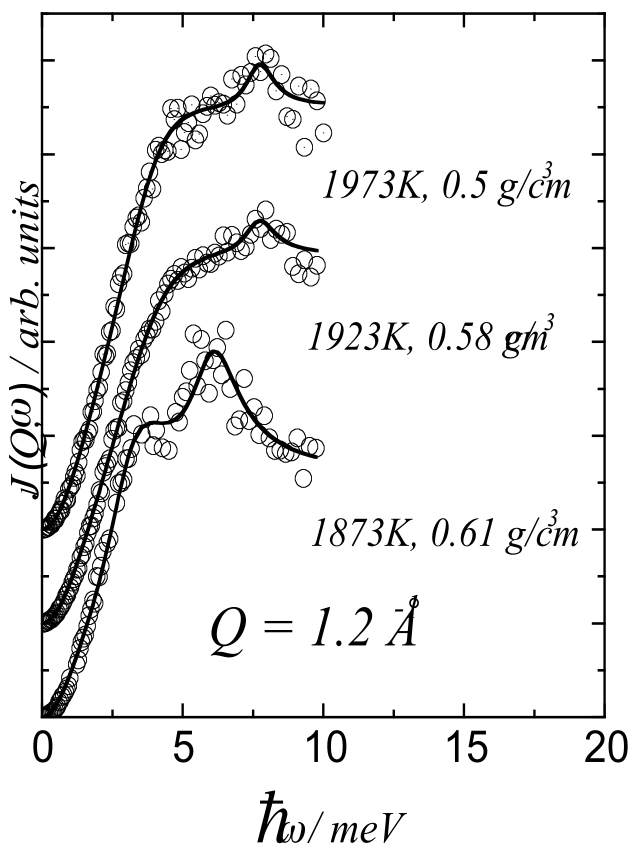

W.-C. Pilgrim et al., J. Non-Cryst. Sol. **250-252**, 154 (1999)

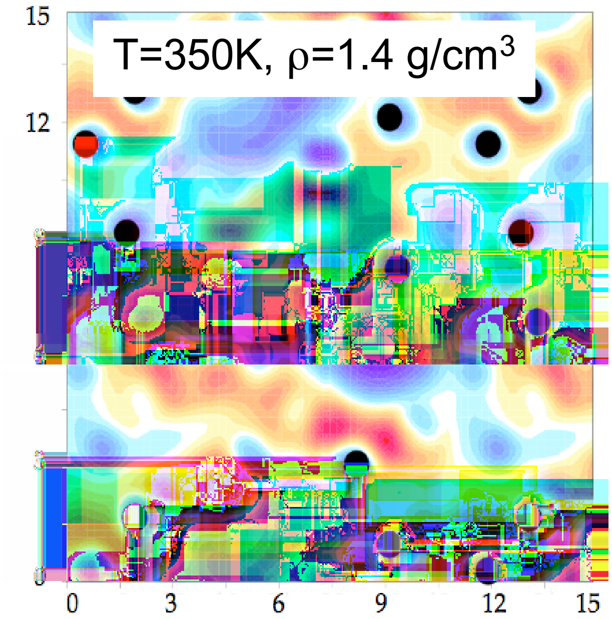

$T=350\text{K}, \rho=1.4\ \text{g/cm}^3$

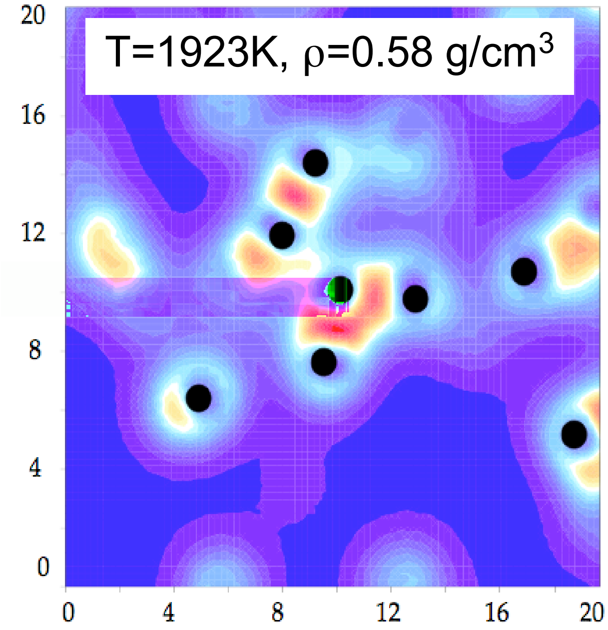

$T=1923\text{K}, \rho=0.58\ \text{g/cm}^3$

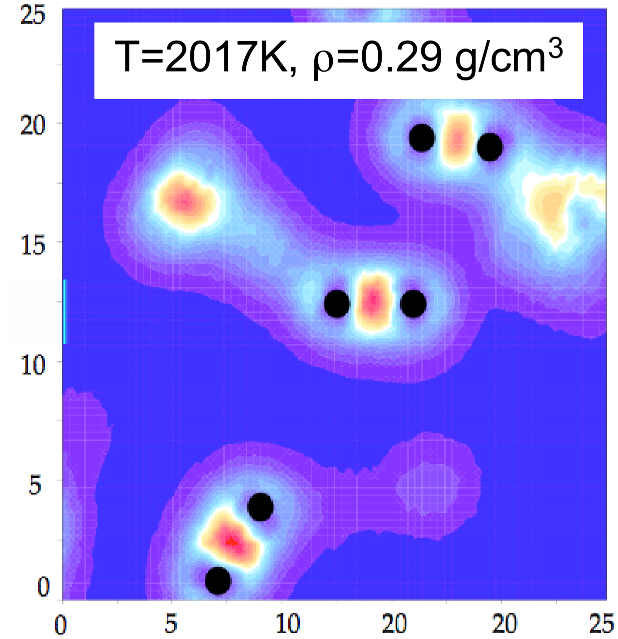

$T=2017\text{K}, \rho=0.29\ \text{g/cm}^3$

M. Ross, L. H. Yang and W.-C. Pilgrim, 2006 (to be published)

Mercury: The ground state of the atom arises from a closed $6s^2$ shell electronic configuration.

The interaction potential between two mercury atoms is thus generally regarded as acting between highly polarizable closed shell systems involving very little electronic density migration from the partners. In this sense, mercury vapor has been denoted “pseudo-helium“.

Pure dispersion forces in Hg-vapor?

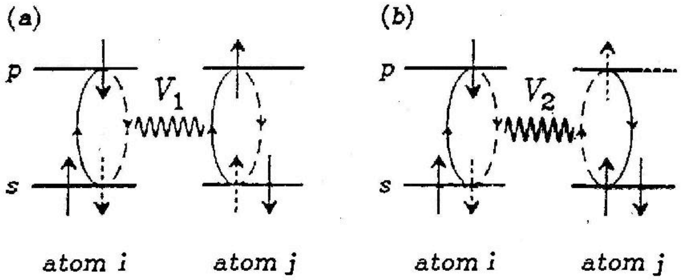

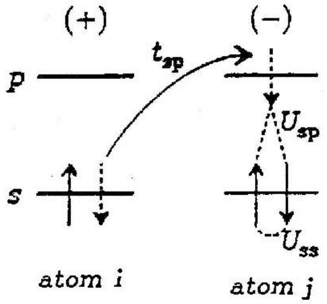

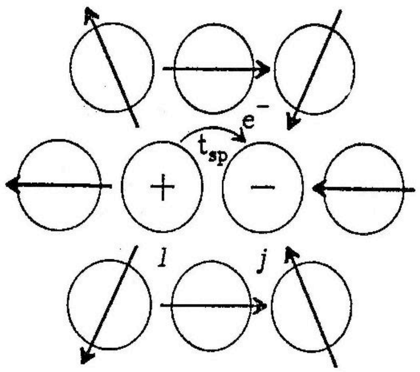

Anisotropy of polarizability

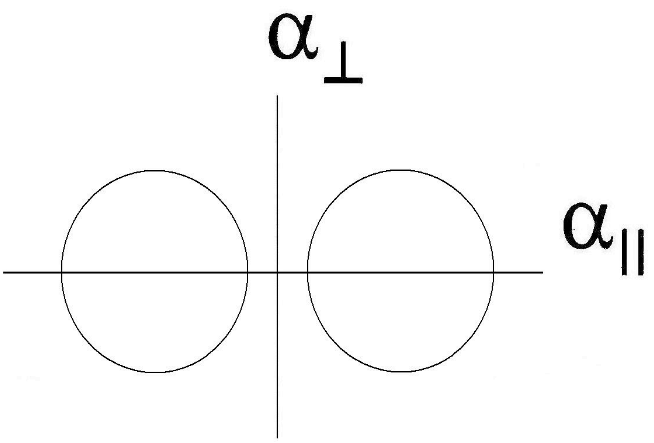

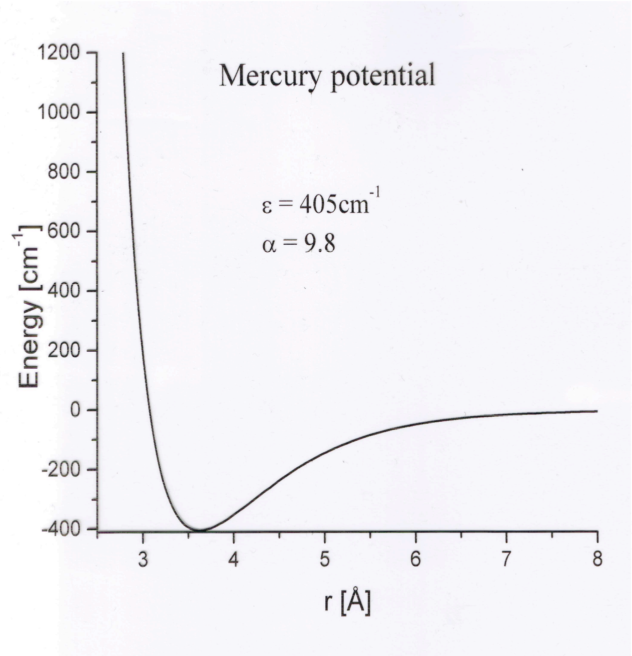

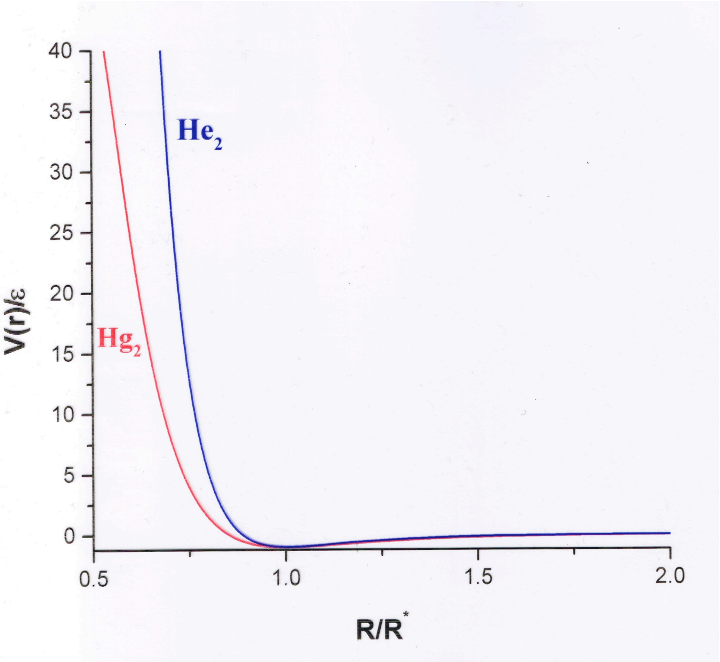

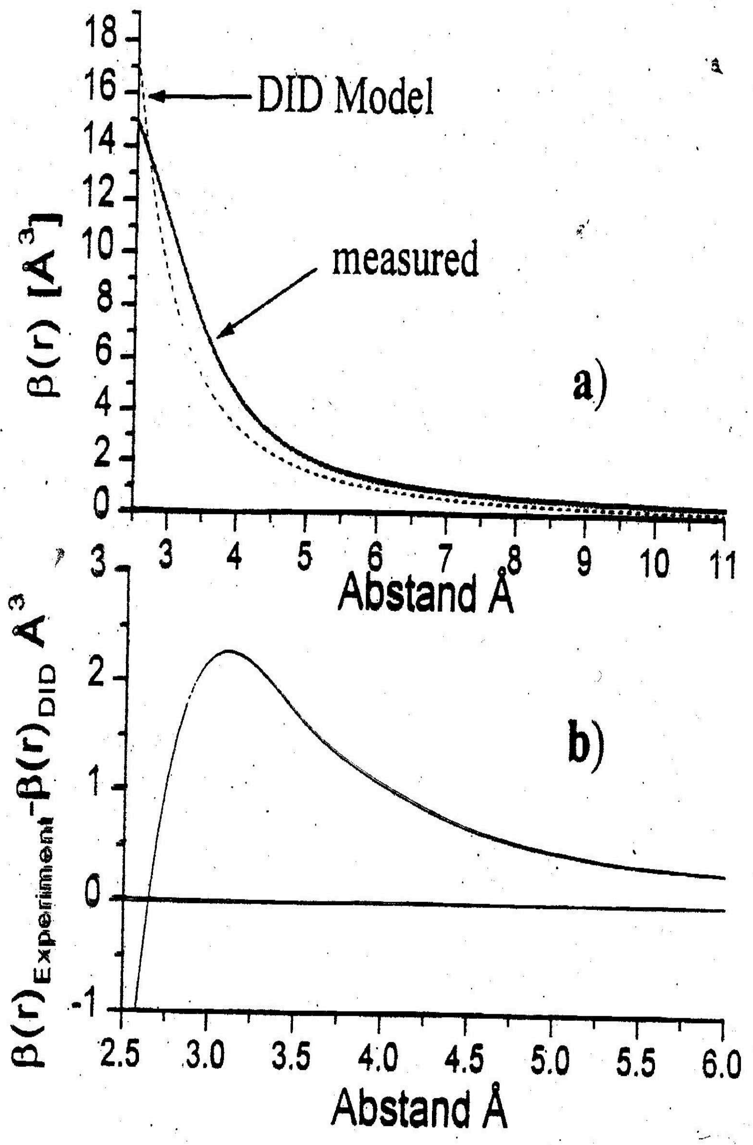
DID Model
measured
a)
β(r) [Å^3]
18
16
14
12
10
8
6
4
2
0
3
4
5
6
7
8
9
10
11
Abstand Å
b)
β(r)$_{Experiment}$-β(r)$_{DID}$ Å^3
3
2
1
0
-1
2.5
3.0
3.5
4.0
4.5
5.0
5.5
6.0
Abstand Å

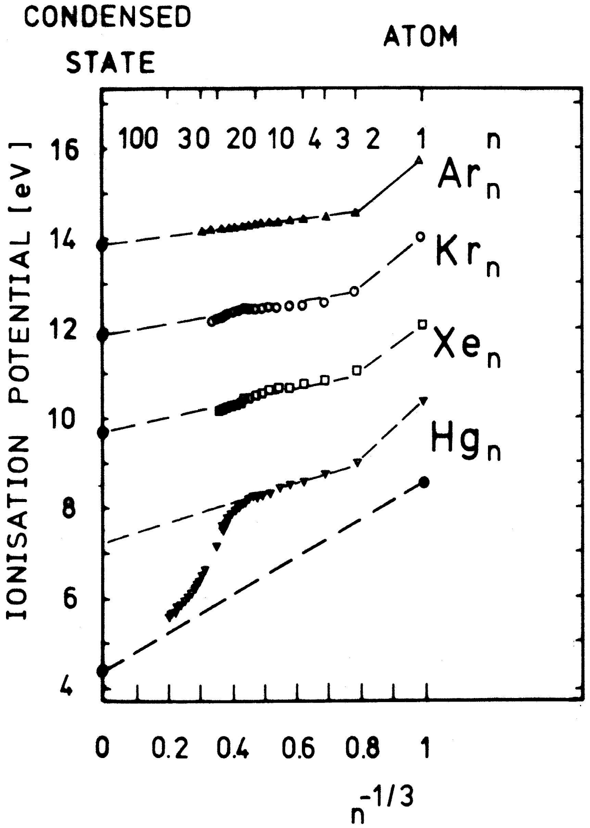
CONDENSED
STATE
ATOM
IONISATION POTENTIAL [eV]
100 30 20 10 4 3 2 1 n
Ar$_n$
Kr$_n$
Xe$_n$
Hg$_n$
16
14
12
10
8
6
4
0 0.2 0.4 0.6 0.8 1
$n^{-1/3}$

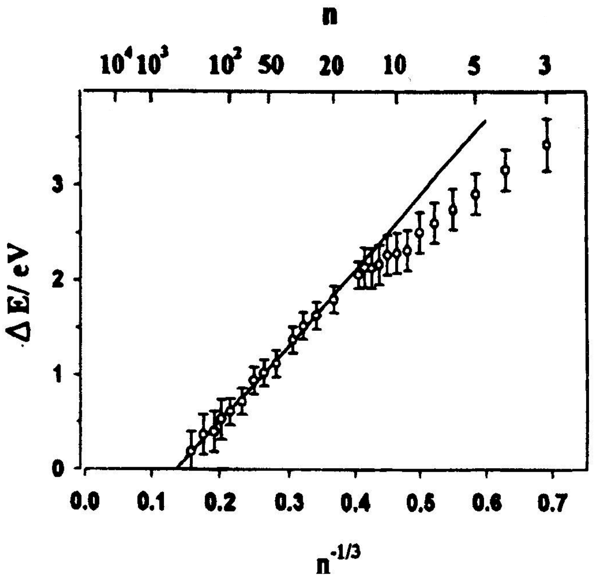
n
10^4 10^3 10^2 50 20 10 5 3
ΔE/ eV
3
2
1
0
0.0 0.1 0.2 0.3 0.4 0.5 0.6 0.7
$n^{-1/3}$

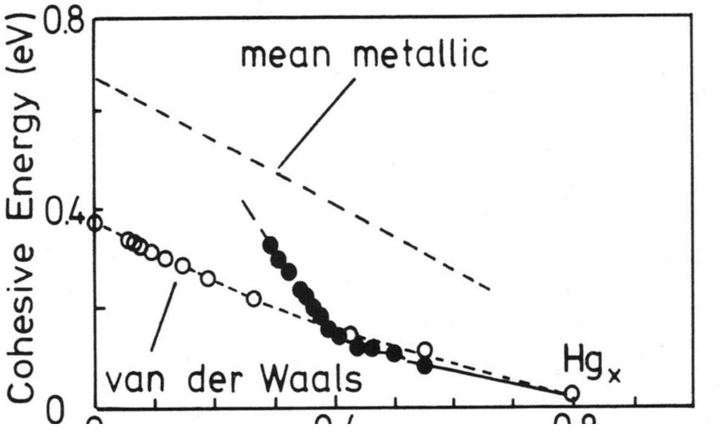
Cohesive Energy (eV)
0.8
0.4
0
mean metallic
van der Waals
Hg$_x$

Mercury

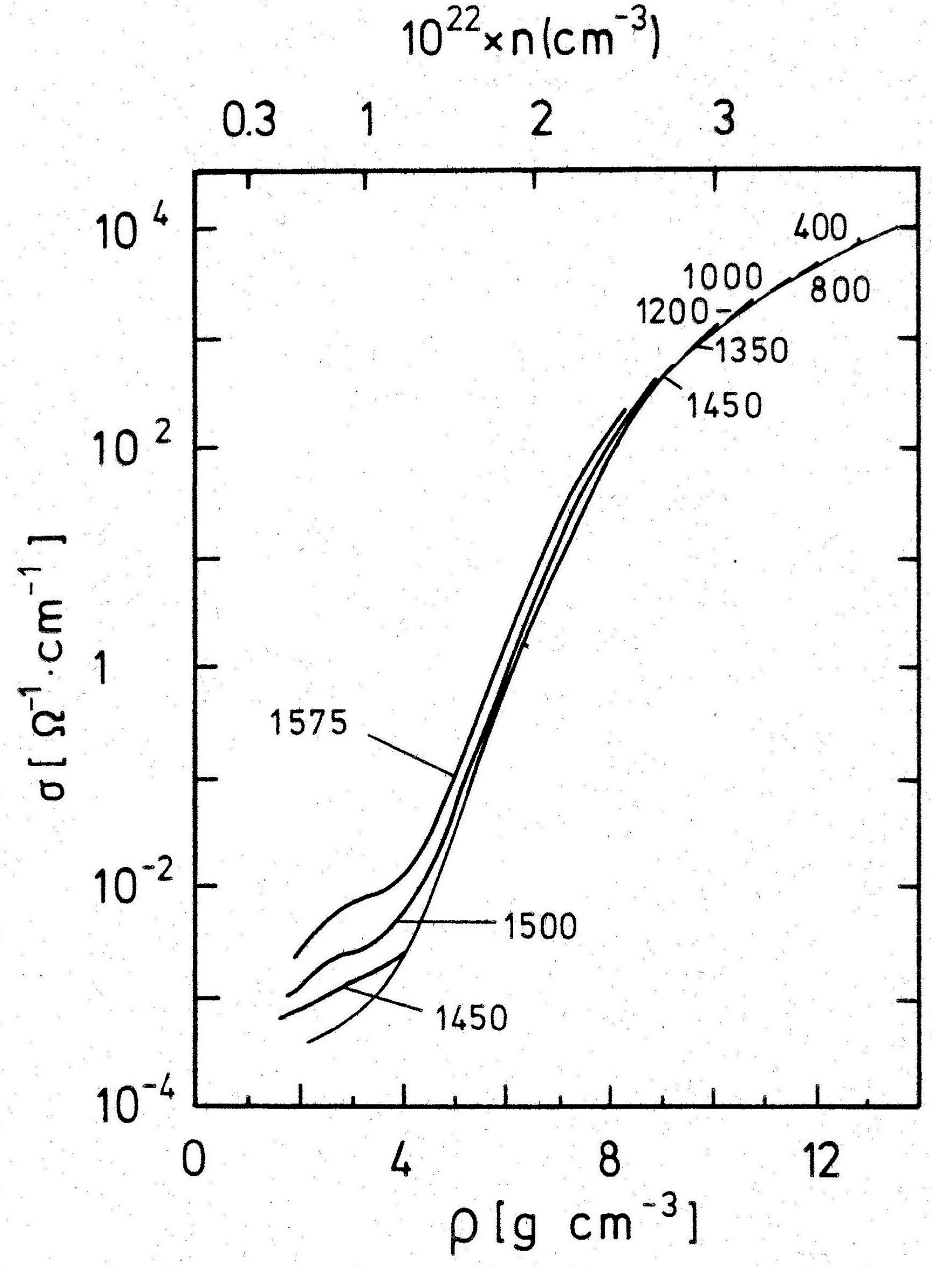

$10^{22} \times n (cm^{-3})$
0.3
1
2
3
10^4
10^2
1
10^{-2}
10^{-4}
$\sigma [\Omega^{-1} \cdot cm^{-1}]$
400
1000
800
1200
1350
1450
1575
1500
1450
0
4
8
12
$\rho [g\ cm^{-3}]$

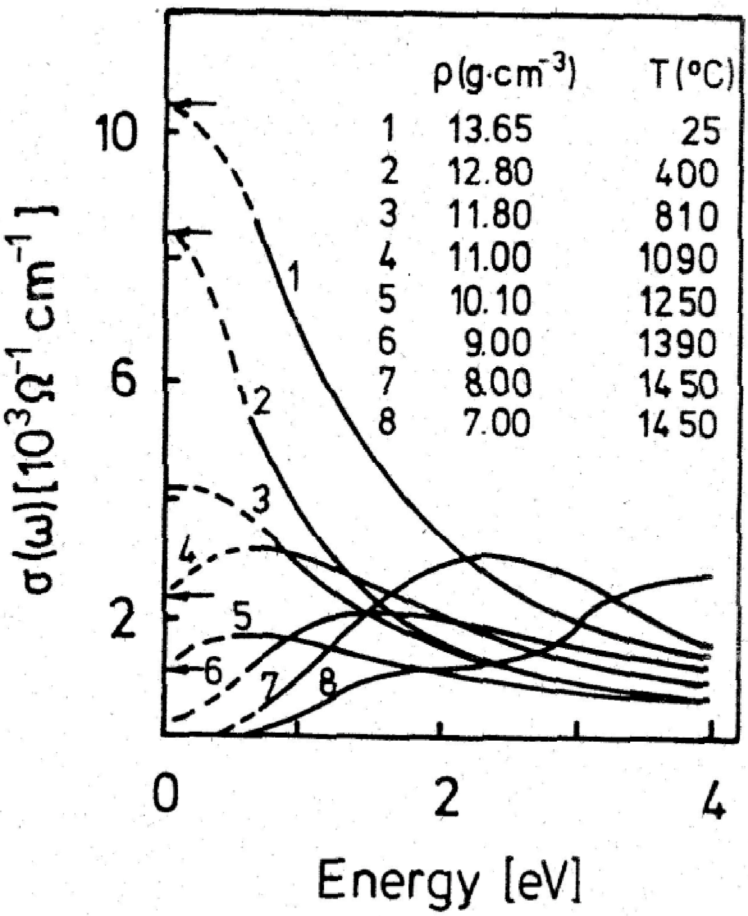

$$B = 2N_i I$$

$$I = \int \Phi_{i+1}\, \Delta v\, \Phi_i\, d^3x$$

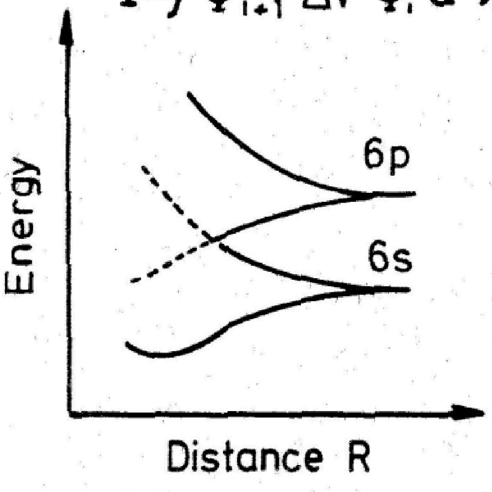

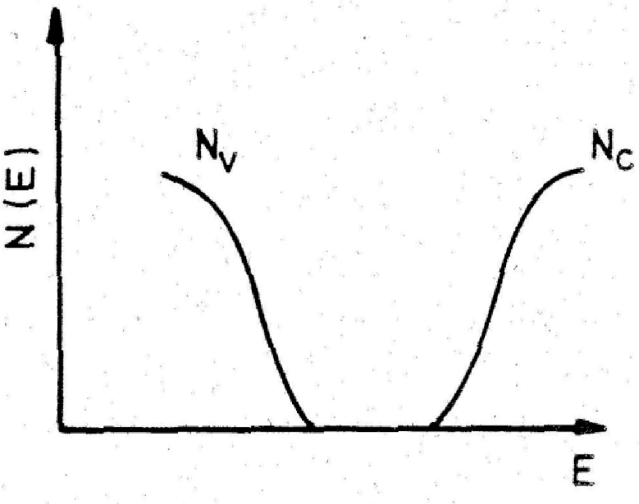

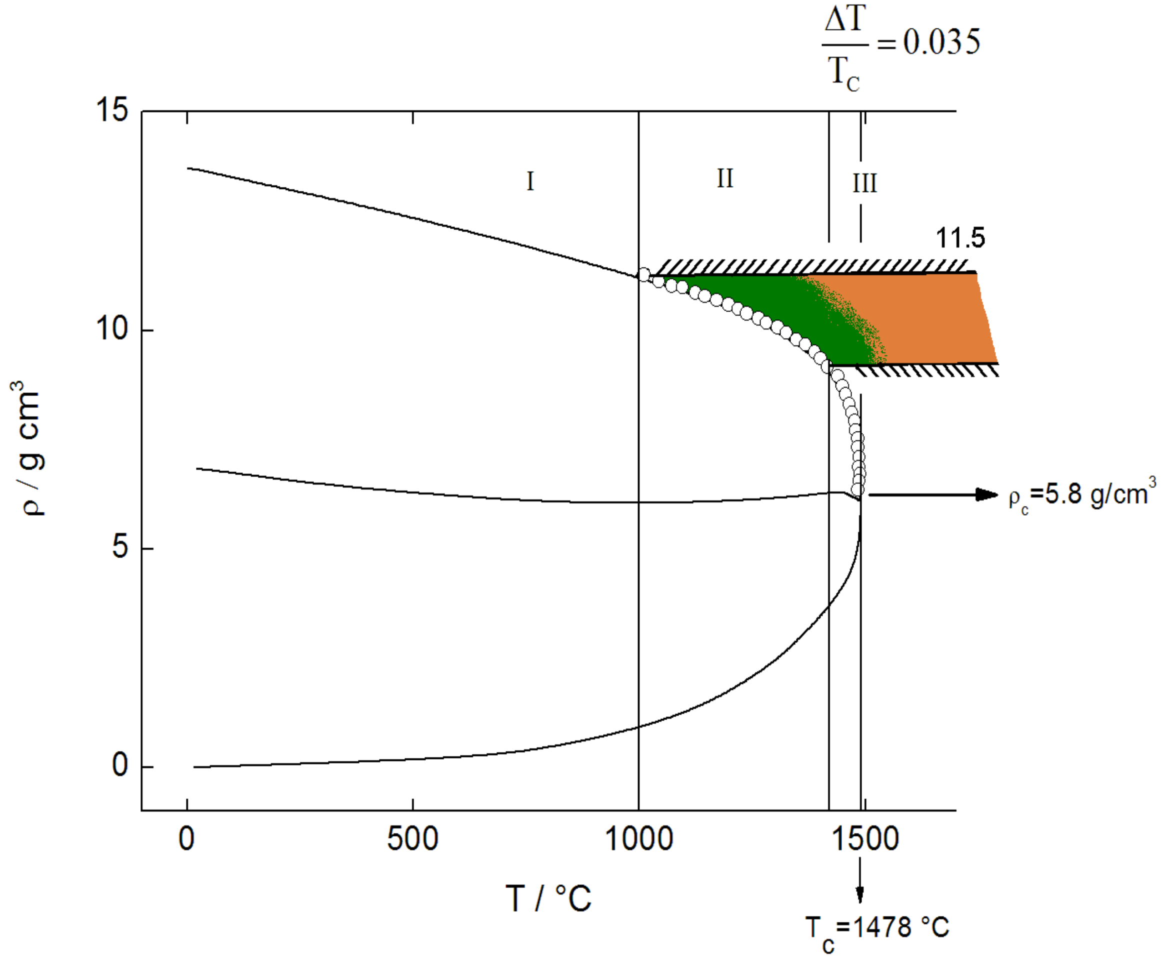
$\frac{\Delta T}{T_C} = 0.035$
15
10
5
0
ρ / g cm^3
I
II
III
11.5
ρ_c=5.8 g/cm^3
0
500
1000
1500
T / °C
T_C=1478 °C

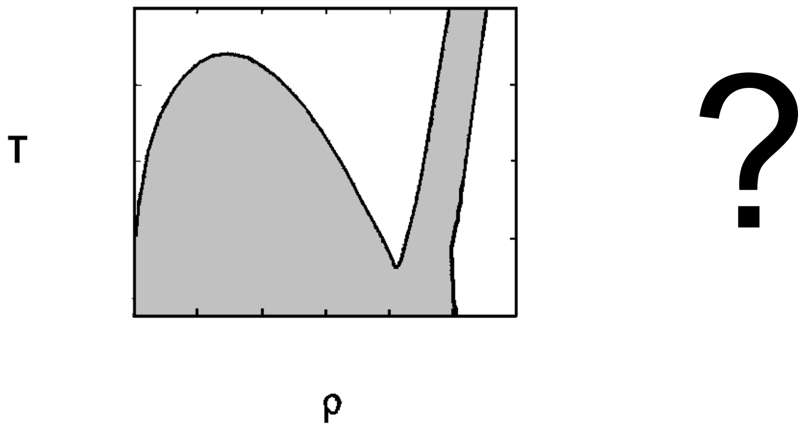
T
ρ
?

Experimental observations between 11 g/cm^3 and 9 g/cm^3 [σ, $\sigma(\omega)$, K, c_S, C_V, S(Q,ω), sound absorption and small- and wide angle scattering] are consistent with the assumption that in this range “metallic clusters” coexist with “nonmetallic fluid regions”.

Evidence for heterophase fluctuations

I.) Static Structure factor

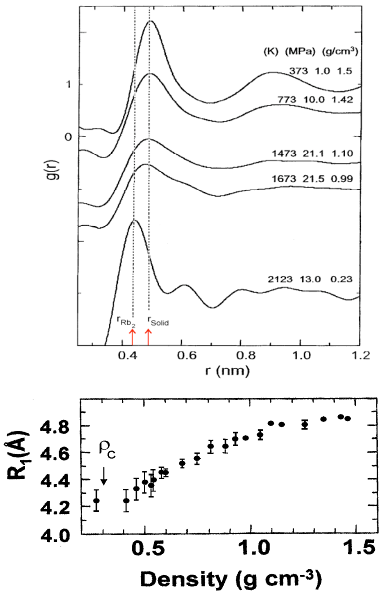

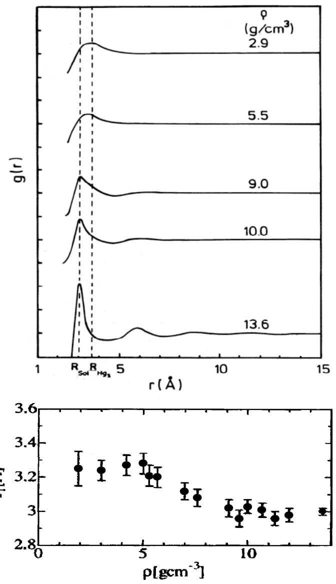

K. Matsuda et al., J. Non-Cryst. Sol. in press (2006)

Inui et al., PRB **68**, 094108 (2003)

II.) Dynamic Structure factor

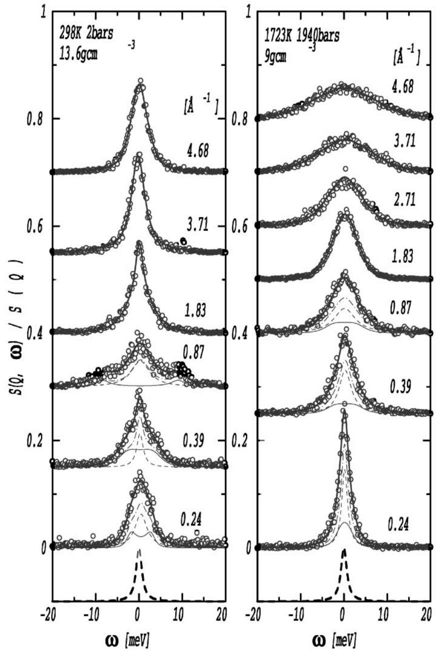

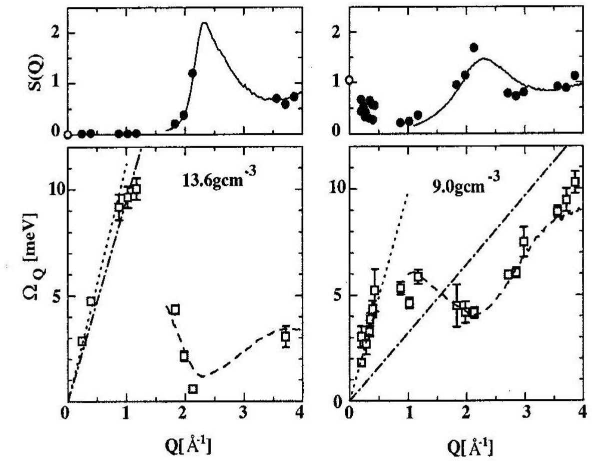

D. Ishikawa et al., PRL **93**, 097801 (2004)

III.) Timescale of structural relaxation

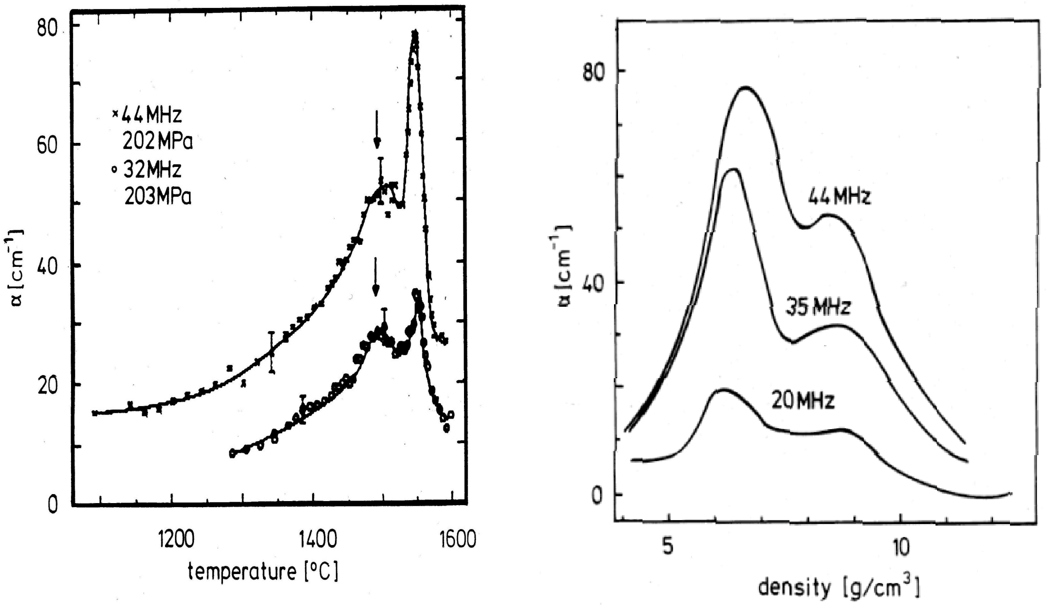

H. Kohno and M. Yao, J. Phys.: Cond. Matt. **13**, 10293 (2001)

IV.) Small angle scattering

M. Inui and K. Tamura
Zeitschr. für Physik. Chemie **217**, 1045 (2003)

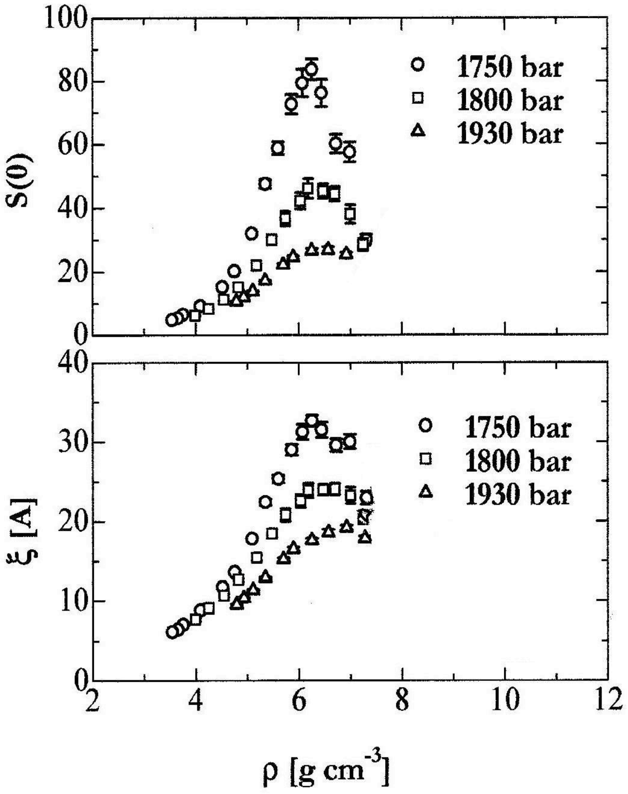

V.) Specific Heat

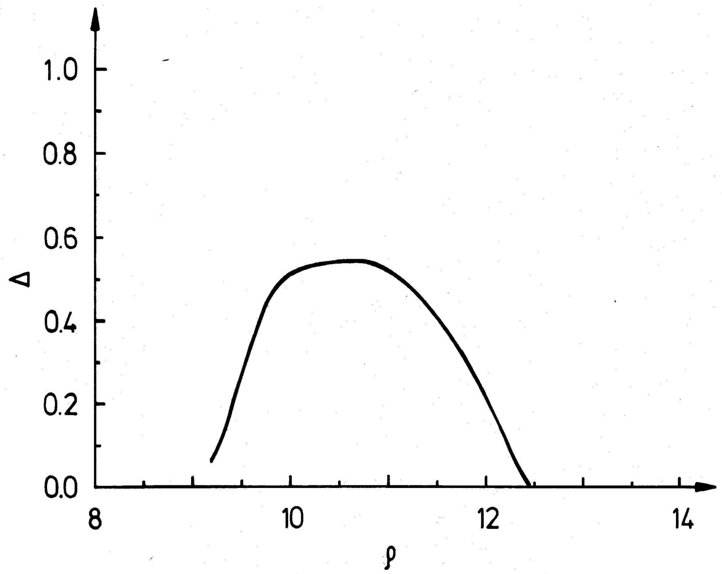

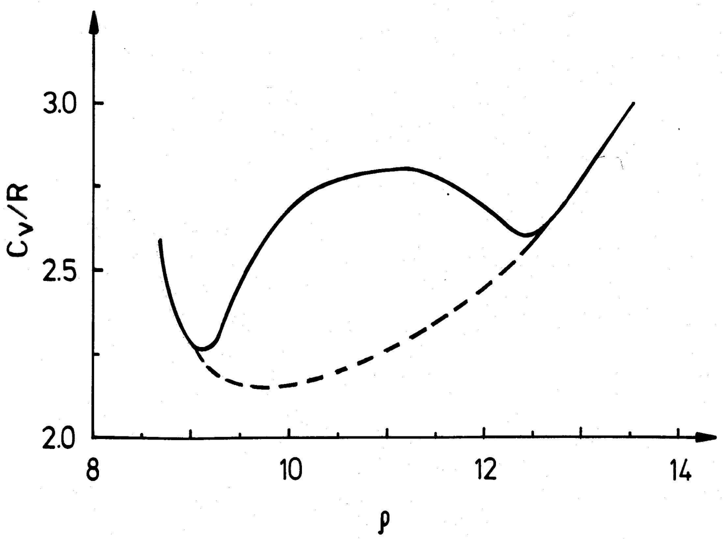

M. Levin and R. W. Schmutzler, J. Non-Cryst. Sol. **61** and **62**, 83 (1984)

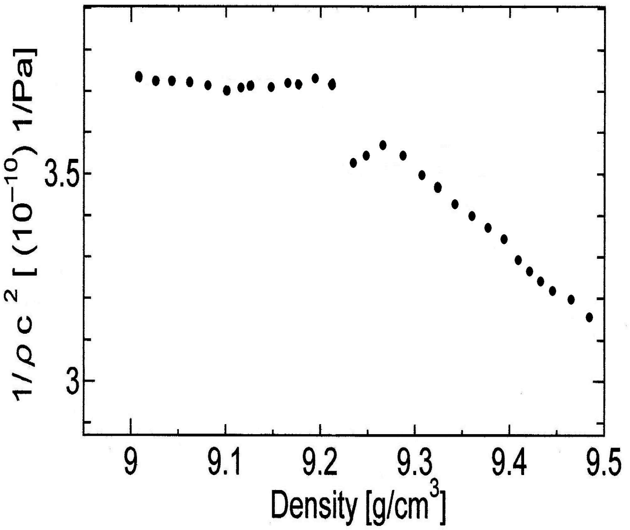

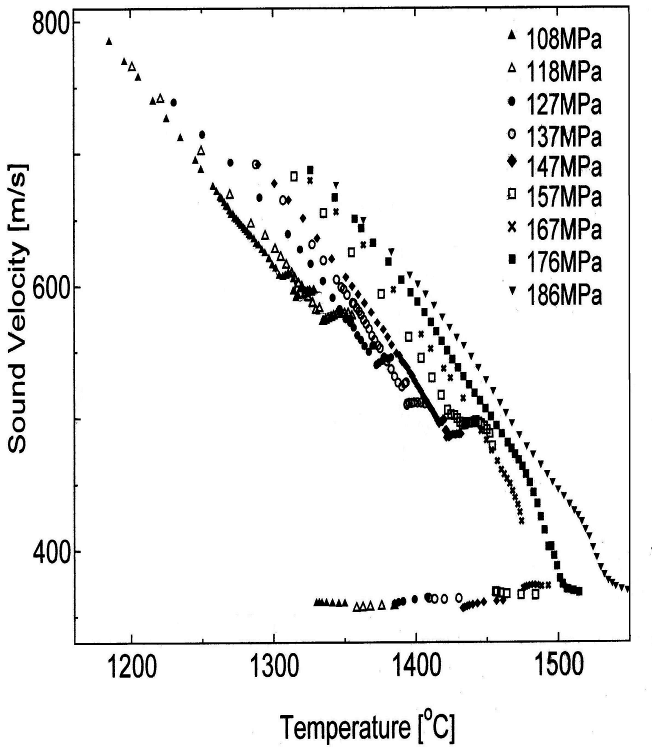

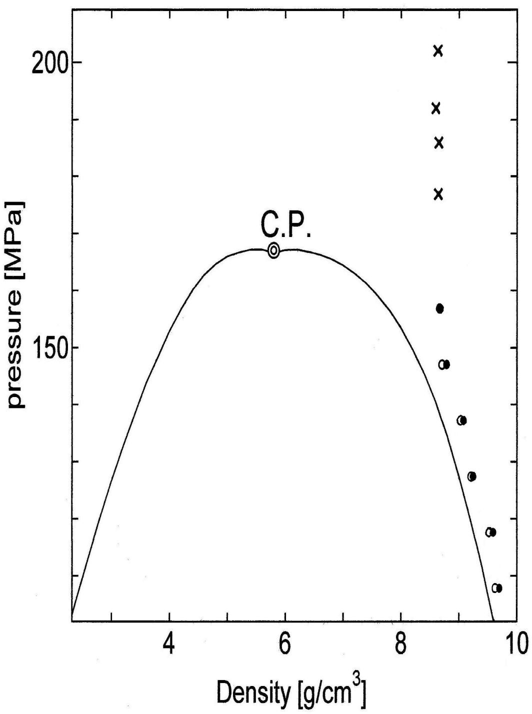

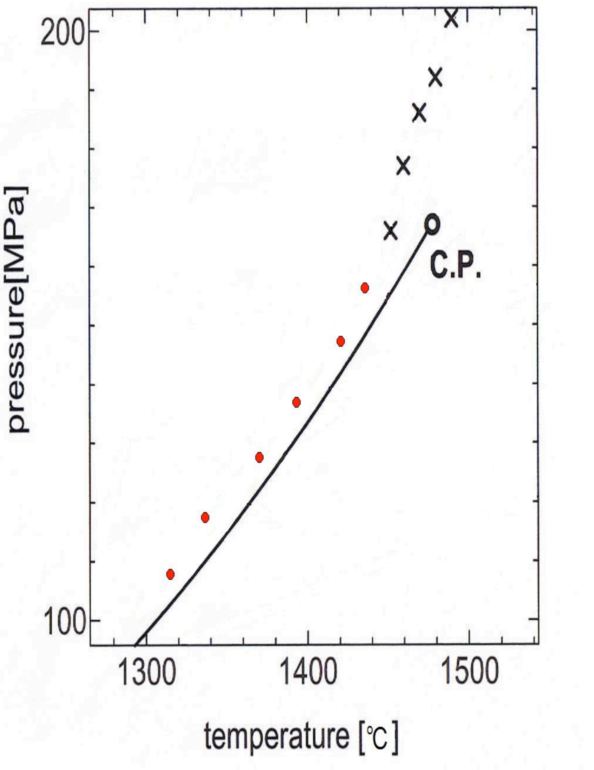

H. Kayikawa et al., J. Non-Cryst. Sol. In press (2006) (LAMXII)

Surface Induced Transitions

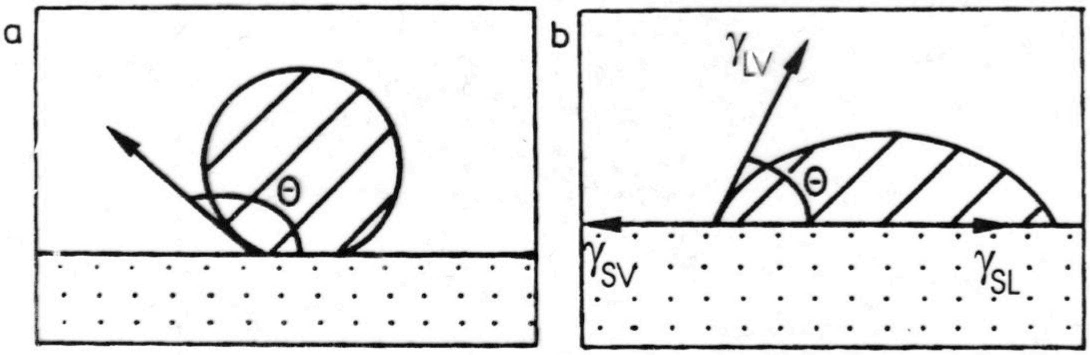

⁙ solid
▨ liquid
☐ vapour

Young‘s equation:

[redacted]

For mercury on Saphire, θ is at room temperature far beyond 90°C.

A convenient measure of the adsorption strength is the ratio of the depth of the potential wells that describe the molecular interactions between substrate-adsorbate (u_{sa}) and adsorbate-adsorbate (V_{aa}). To observe the wetting transition the ratio u_{sa}/V_{aa} needs to be small.

Non-wetting:

$$\gamma_{SV} - \gamma_{SL} < \gamma_{LV}$$

$$\gamma_{LV} \sim (T_C - T_C)^{2\upsilon} \sim (T_C - T)^{1.3}$$

$$\gamma_{SV} - \gamma_{SL} \sim (n_L - n_V)\ \mathrm{surf} \sim (T_C - T)^{\beta 1} \sim (T_C - T)^{0.8}$$

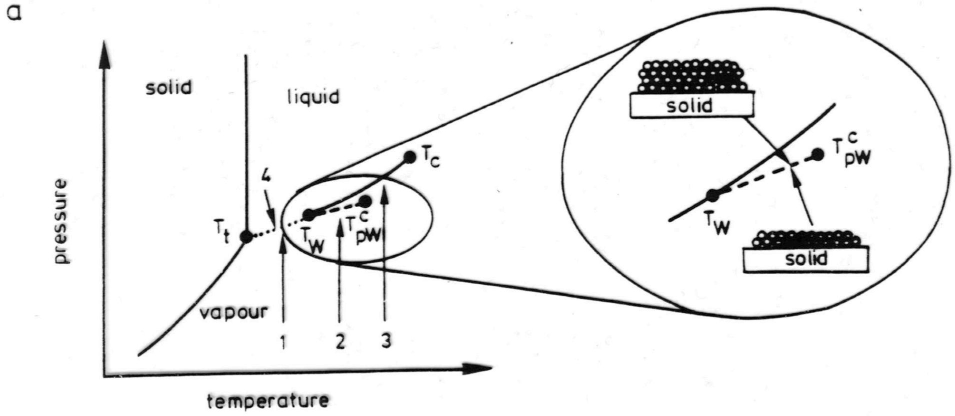

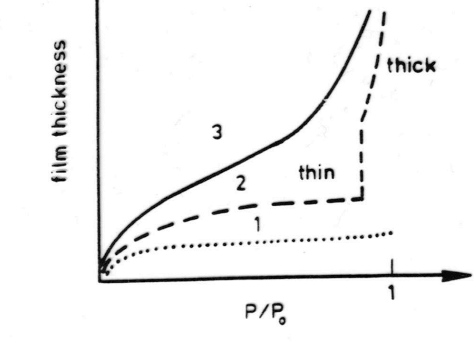

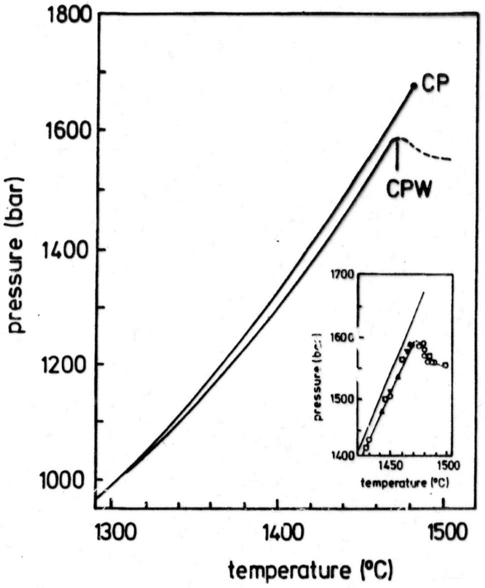
1800
1600
1400
1200
1000
pressure (bar)
1300
1400
1500
temperature (°C)
CP
CPW
1700
1600
1500
1400
pressure (bar)
1450
1500
temperature (°C)

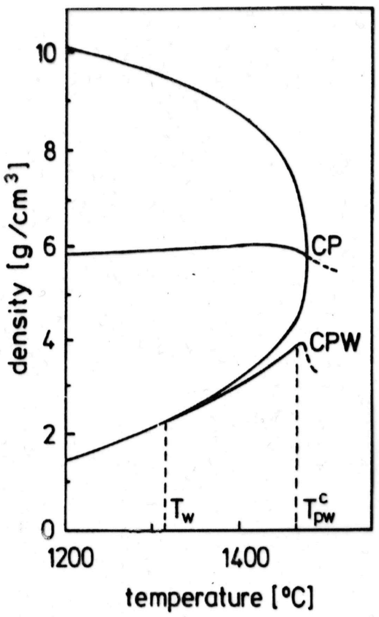
10
8
6
4
2
0
density [g/cm^3]
1200
1400
temperature [°C]
CP
CPW
T_w
T_{pw}^c

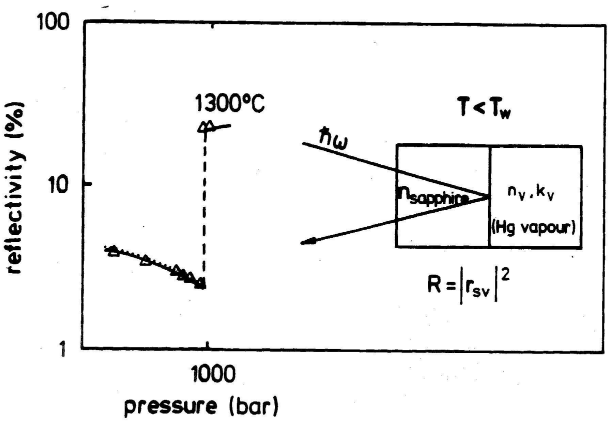
100
10
1
reflectivity (%)
1000
pressure (bar)
1300°C
T < T_w
$\hbar\omega$
$n_{sapphire}$
n_V, k_V
(Hg vapour)
$R = |r_{SV}|^2$

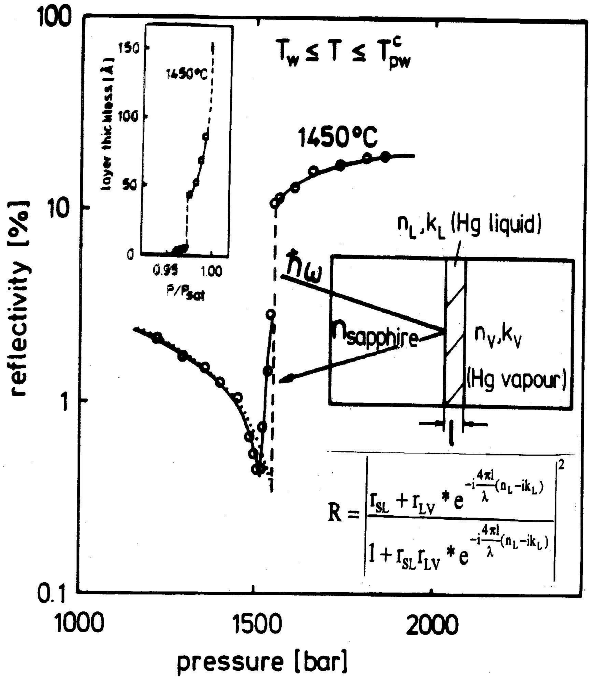
100
10
1
0.1
reflectivity [%]
1000
1500
2000
pressure [bar]
$T_w \leq T \leq T_{pw}^c$
1450°C
layer thickness [Å]
150
100
50
0
1450°C
0.95
1.00
P/P_{sat}
n_L, k_L (Hg liquid)
$\hbar\omega$
$n_{sapphire}$
n_V, k_V
(Hg vapour)
l
$R = \left| \frac{r_{SL} + r_{LV} * e^{-i\frac{4\pi l}{\lambda}(n_L - ik_L)}}{1 + r_{SL} r_{LV} * e^{-i\frac{4\pi l}{\lambda}(n_L - ik_L)}} \right|^2$

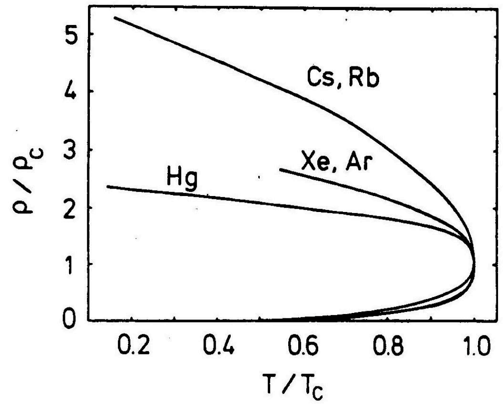
Cs, Rb
Xe, Ar
Hg
ρ / ρ_c
5
4
3
2
1
0
0.2
0.4
0.6
0.8
1.0
T / T_c

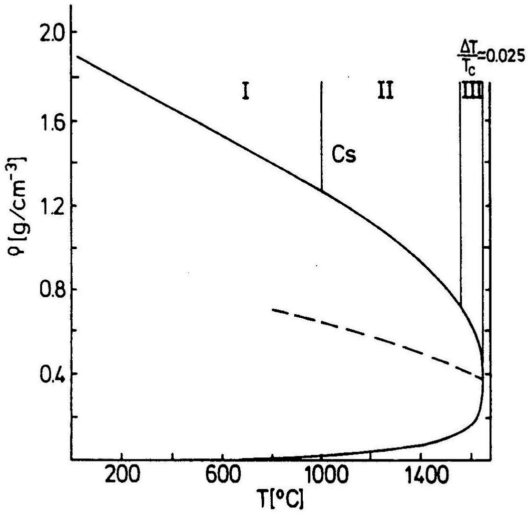
ΔT/T_c ≈ 0.025
I
II
III
Cs
ρ [g/cm⁻³]
2.0
1.6
1.2
0.8
0.4
200
600
1000
1400
T[°C]

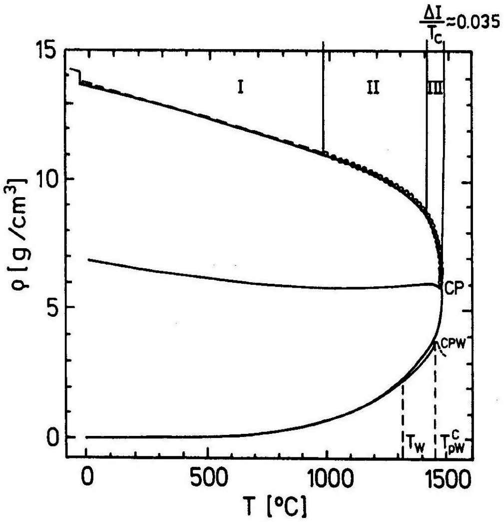
ΔT/T_c ≈ 0.035
I
II
III
CP
CPW
T_W
T^C_pW
ρ [g/cm³]
15
10
5
0
0
500
1000
1500
T [°C]

Critical Phenomena

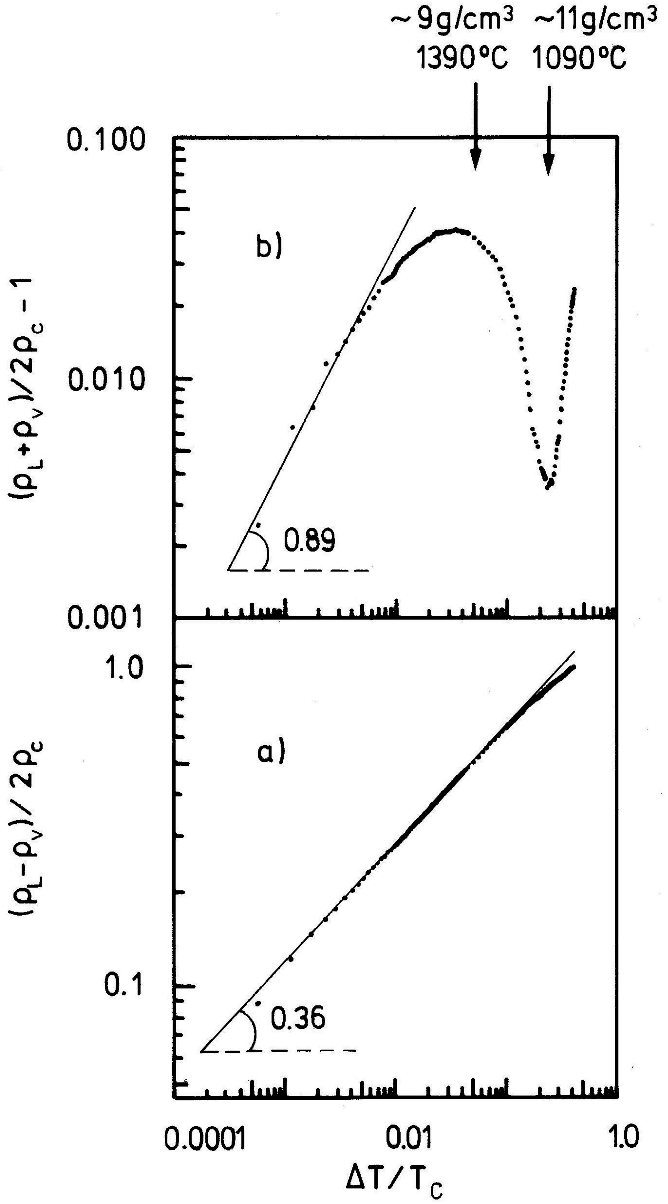

$$\rho_{L,V} = \rho_c \pm B\left(\frac{\Delta T}{T_c}\right)^{\beta} + A\left(\frac{\Delta T}{T_c}\right)^{(1-\alpha)} + ---$$

$$\frac{\rho_L-\rho_V}{2\rho_c} = B\left(\frac{\Delta T}{T_c}\right)^{\beta}$$

$$\rho_d = \frac{\rho_L+\rho_V}{2\rho_c} = 1 + D\left(\frac{\Delta T}{T_c}\right)^{(1-\alpha)}$$

$$\beta^{\mathrm{eff}}_{L,V} = \frac{\partial \ln|\rho_{L,V}-\rho_d|}{\partial \ln\left(\frac{\Delta T}{T_c}\right)}$$

$$\beta^{\mathrm{assym}}_{L,V} = \lim_{\frac{\Delta T}{T_c}\to 0} \beta^{\mathrm{eff}}_{L,V}$$

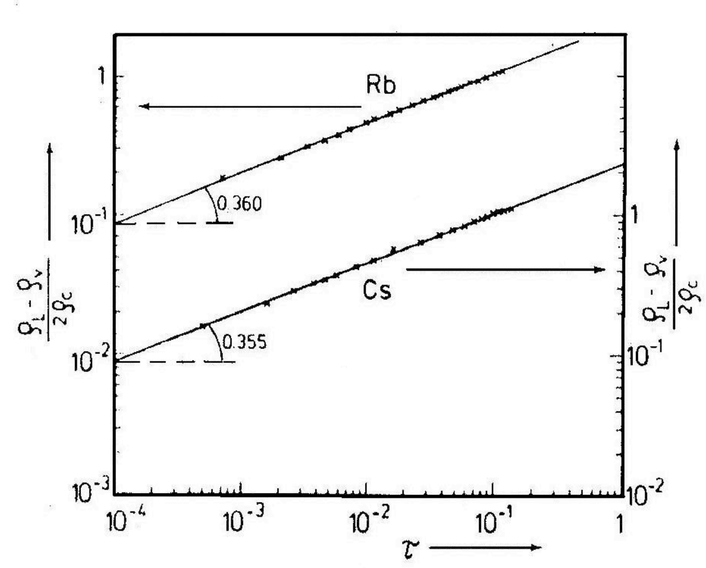

Rb
Cs
0.360
0.355
$\frac{\rho_L - \rho_v}{2\rho_c}$
$\frac{\rho_L - \rho_v}{2\rho_c}$
1
10^{-1}
10^{-2}
10^{-3}
1
10^{-1}
10^{-2}
10^{-4}
10^{-3}
10^{-2}
10^{-1}
1
τ

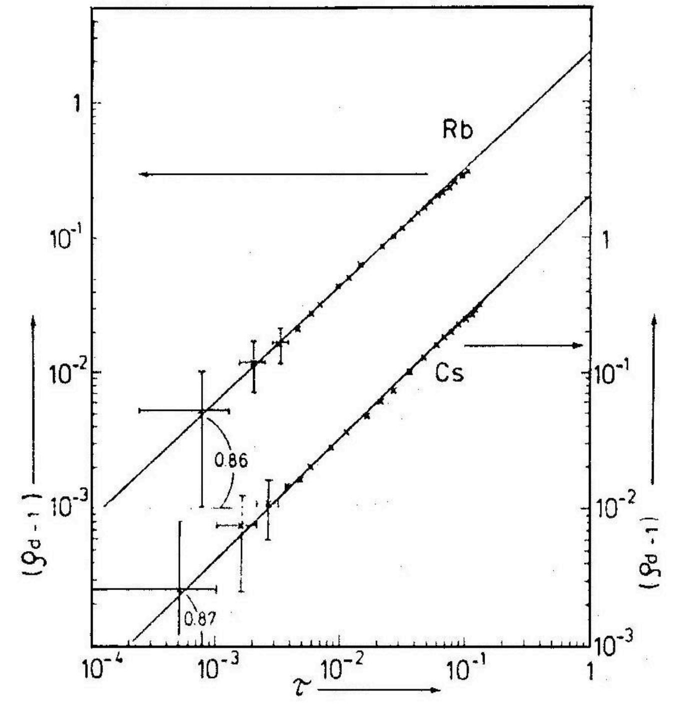

Rb
Cs
0.86
0.87
$(\rho_d - 1)$
$(\rho_d - 1)$
1
10^{-1}
10^{-2}
10^{-3}
1
10^{-1}
10^{-2}
10^{-3}
10^{-4}
10^{-3}
10^{-2}
10^{-1}
1
τ